

# Sensor Biases Effect on the Estimation Algorithm for Performance-Seeking Controllers

Martín D. España\*

National Research Council/NASA Dryden Flight Research Facility, Edwards, California 93523

The performance-seeking-control algorithm (PSC) is designed to continuously optimize the performance of propulsion systems. The PSC uses a nominal model of the propulsion system and estimates, in flight, the engine deviation parameters (EDPs) characterizing engine deviations with respect to nominal conditions. In practice, the measurement biases (or model uncertainties) may prevent the estimated EDPs from reflecting the engine's actual off-nominal condition. This factor has a direct impact on the PSC scheme exacerbated by the open-loop character of the algorithm. An observability analysis shows that the biases cannot be estimated together with the EDPs. Moreover, biases and EDPs turn out to have equivalent effects on the measurements, leaving it undecided whether the estimated EDPs represent the actual engine deviation or whether they simply reflect the measurement biases. In this article, the effects produced by unknown measurement biases over the estimation algorithm are evaluated. This evaluation allows for identification of the most critical measurements for application of the PSC algorithm to an F100 engine.

## Nomenclature

$A, B, C, D, L, M$	= state variable model matrices	$Y, y$	= measured and incremental measured output vector, respectively
AAHT	= area adder high-pressure turbine deviation parameter, in. <sup>2</sup>	$Y_{aux}, y_{aux}$	= unmeasured and incremental unmeasured output vectors, respectively
AJ	= nozzle throat area, in. <sup>2</sup>	$Z, z$	= output vector and incremental output vector, respectively
BLD	= bleed airflow, lb/s	$\gamma, \nu$	= bias vector in the output and input measurements, respectively
CIVV	= compressor inlet variable guide vane angle, deg	$\eta$	= engine deviation parameters vector
DEHPT	= high-pressure turbine efficiency deviation parameter, percent	$(\omega_x, \omega_\eta), \rho$	= process and measurement noise of the Kalman filter model, respectively
DELPT	= low-pressure turbine efficiency deviation parameter, percent		
DINL	= inlet drag, lb		
DWFAN	= fan airflow component deviation parameter, lb/s	<i>Subscripts</i>	
DWHPC	= high-pressure compressor airflow deviation parameter, lb/s	ap	= apparent
FTIT	= fan turbine inlet temperature, °F	aux	= auxiliary
$G_y, G_{aux}, H_y, H_{aux}$	= gain submatrices of the optimization model	b	= base point
HPX	= power extraction, hp	eq	= equivalent increment
$I_m$	= identity matrix of dimension $m$	<i>Symbols</i>	
$N_1, N_2$	= fan and compressor rotor speed, respectively, rpm	$\mathbb{R}$	= set of real numbers
$P, Q, R$	= estimate, process, and measurement covariance matrices, respectively	$\in$	= is a member of
$P_{amb}$	= ambient pressure, lb/in. <sup>2</sup>	$[ ]^T$	= matrix transpose
PB	= burner pressure, lb/in. <sup>2</sup>	$\hat{\phantom{x}}$	= estimated variable
PS	= static pressure, lb/in. <sup>2</sup>		
PT	= total pressure, lb/in. <sup>2</sup>		
RCVV	= rear compressor variable vanes, deg		
TMT	= composite turbine metal temperature, °F		
TT	= total temperature, °F		
$x$	= incremental state variable		

## Introduction

THE objective of the performance-seeking-control algorithm (PSC) is to operate a (turbofan engine-based) propulsion system as closely as possible to its optimum steady-state working condition without compromising reliability and operability.<sup>1–4</sup> Three different operating modes are sought corresponding, respectively, to three different optimization criteria. They are 1) minimum fuel consumption, 2) minimum temperature of the hot section of the engine (also called extended engine life mode), and 3) maximum thrust.

The PSC system was implemented on the NASA F-15 research aircraft, which is powered by two F100 derivative (PW1128) afterburning turbofan engines.<sup>2</sup> The aircraft was modified with a full-authority digital electronic engine control (DEEC) system. The DEEC provides basic open-loop scheduling and closed-loop feedback control of the propulsion variables.<sup>2</sup> Its software was modified to accommodate PSC trim commands without altering the basic control functions. The PSC system testing at subsonic flight conditions<sup>2</sup> shows up to 15% increases in thrust, up to 100°R reductions in the turbine

Presented as Paper 93-1823 at the AIAA/SAE/ASME/ASCE 29th Joint Propulsion Conference and Exhibit, June 28–30, 1993; received July 8, 1993; revision received Jan. 15, 1994; accepted for publication Jan. 15, 1994. Copyright © 1993 by M. D. España. Published by the American Institute of Aeronautics and Astronautics, Inc., with permission.

\*Research Associate, Propulsion Branch, P.O. Box 273, M/S D-2002. Member AIAA.

temperature, and between 1–2% savings in thrust specific fuel consumption (TSFC). Preliminary flight evaluations of the PSC algorithm at supersonic flight conditions have been performed indicating thrust increases of approximately 10%, and a TSFC reduction of approximately 9%.<sup>5</sup>

The optimization is based on a steady-state model of the entire propulsion system (integrating the inlet, the engine, and the nozzle) called *the optimization model*. A fixed model of the propulsion system would not be able to account for the significant changes experienced by the engine during its life span (engine deterioration) or for the differences from aircraft-to-aircraft resulting from manufacturing variability. As such, a mechanism for the adaptation of the engine model is required. For this purpose, the optimization model includes a set of adjustable parameters: the engine deviation parameter (EDPs), characterizing the current engine operating condition. In-flight estimation of the EDPs gives an adaptive character to the PSC. The estimation is performed with a Kalman filter (KF) based on a reduced-order linear dynamic model of the engine called *the estimation model*.

The algorithm is expected to work well when the estimated values of the EDPs actually represent the current off-nominal conditions of the engine. However, it has been shown during flight testing<sup>2</sup> that the estimated EDPs may not correspond to known levels of engine deterioration. This fact is attributed to other sources of model-engine mismatch not accounted for by the EDPs. Poor EDP estimates translate into an inadequate prediction (provided by the optimization model) of the engine's behavior, which in turn may degrade the optimization process. Given the importance of the estimation algorithm in the overall adaptive PSC scheme, the effects of measurement biases (or other model inaccuracies) over the optimization process need to be evaluated.

In this article, we show that with the present measurement system unknown biases cannot be estimated independently of the EDPs and, consequently, that their effects may not be compensated for. A sensitivity approach is used to quantify the biases' influence over the predictions of the steady-state optimization model. The study allows us to decide, for the F100 engine, which measurement biases have more influence over the estimation process and which estimates are affected the most by the biases.

### Background and Problem Formulation

Figure 1 is an F100 engine diagram showing the location of the DEEC instrumentation, the DEEC-calculated variables, and the parameters calculated by the PSC algorithm. Figure 2 shows an information flow diagram of the PSC algorithm. The PSC consists of an estimation algorithm, which updates the EDPs' estimates, and an open-loop model-based optimization control law. Each process—estimation and optimization—is based on a different set of local models of the propulsion system. The current local model for each process

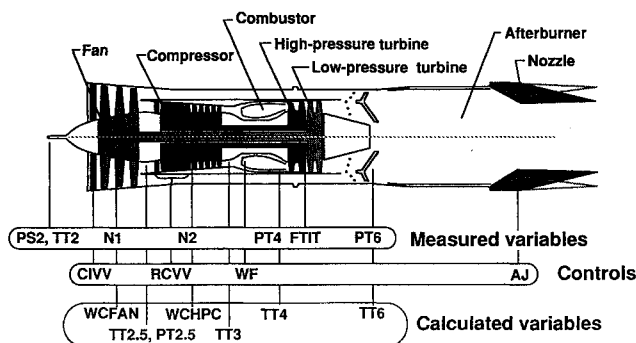


Fig. 1 F100 engine and sensor locations of sensors. 2 = fan inlet, 2.5 = compressor inlet, 3 = compressor discharge, 4 = high-pressure turbine inlet, 4.5 = low-pressure turbine inlet, 6 = afterburner inlet, 7 = nozzle throat.

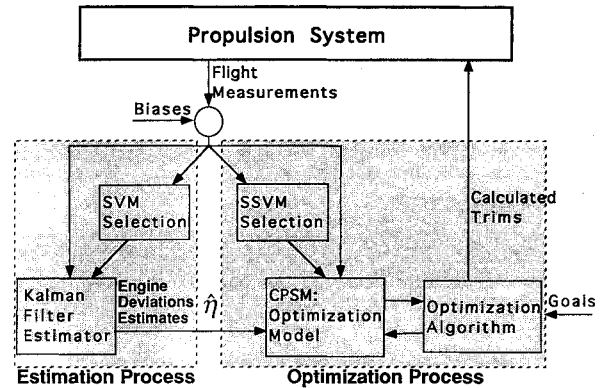


Fig. 2 Flow diagram of the PSC algorithm.

is selected on the basis of flight data. More details on the overall structure of the PSC system can be found in Ref. 2.

The engine model relates the measured input vector  $U$  with the output vector  $Z$  defined as

$$U^T := [WF \ A_j \ CIVV \ RCVV \ HPC \ BLD] \quad (1a)$$

$$Z^T := [Y^T, Y_{aux}^T] \quad (1b)$$

$$Y^T := [N1 \ N2 \ PT4 \ FTIT \ PT6] \quad (1c)$$

$$Y_{aux}^T := [TT6 \ WCFAN \ PT2.5 \ TT2.5 \ TT3 \ TT4 \ WCHPC] \quad (1d)$$

Where  $Y$  is the measured outputs and  $Y_{aux}$  is a set of unmeasured variables required by the optimization process. ( $PT4$  is considered as a measured variable though it is calculated as function of the measure of  $PB$ .)

In order to account for significant deviations with respect to nominal conditions experienced by the engine during its life span (engine deterioration) or for engine-to-engine manufacturing variability, the optimization model includes a set of adjustable parameters called the EDPs denoted as<sup>1-4</sup>

$$\eta^T := [DEHPT \ DELPT \ DWHPC \ DWFAN \ AAHT] \quad (2)$$

For the nominal engine,  $\eta = 0$ . We now define

$$u := U - U_b, \quad y := Y - Y_b \quad \text{and} \quad z := Z - Z_b \quad (3)$$

where  $U_b$ ,  $Y_b$ , and  $Z_b$  are, respectively, the vectors  $U$ ,  $Y$ , and  $Z$  evaluated at some predicted engine trim point called *base point*.

The following linear model has been used<sup>1</sup> to characterize, locally around a base point, the dynamic relationship between the input  $U$  and the measured output  $Y$  for a given off-nominal condition quantified by the time-invariant vector  $\eta$ :

$$\dot{x} = Ax + Bu + L\eta \quad (4a)$$

$$y = Cx + Du + M\eta \quad (4b)$$

Equations (4), called the state variable model (SVM), were developed by Luppold et al.<sup>1</sup> through model order reduction and linearization of the aerothermodynamic equations of the engine. The incremental state variable  $x$  is defined as

$$x^T := [N1 - N1_b, N2 - N2_b, TMT - TMT_b] \quad (5)$$

where  $TMT$  is a composite variable representing the thermal state of the hot section of the engine. Again,  $N1_b$ ,  $N2_b$ , and  $TMT_b$  represent the corresponding variables at the base point. Finally,  $A$ ,  $B$ ,  $C$ ,  $D$ ,  $L$ , and  $M$  are matrices with the appropriate dimensions.

The continuum set of possible base points covering the operation range of a nominal engine for a particular reference flight condition is discretized. The discrete base points are computed using the state of the art propulsion program (SOAPP) which is a detailed model of the whole propulsion system.<sup>6</sup> The reference flight condition used in the present study corresponds to standard day conditions, Mach 0.9, and an altitude of 30,000 ft. By using correction factors, calculated as a function of the total inlet pressure and temperature, the results can be converted to the actual given flight conditions. In this way, the validity of the model can be extended to the whole flight envelope.

#### Estimation Process of the PSC Algorithm

The estimation process is based on a set of local engine linear dynamic models<sup>1,4</sup> represented as

$$\dot{x} = Ax + Bu + L\eta + \omega_x \quad (6a)$$

$$\dot{\eta} = \omega_\eta \quad (6b)$$

$$y = Cx + Du + M\eta + \rho \quad (6c)$$

$\omega_\eta$ ,  $\omega_x$ , and  $\rho$  are centered white noises with positive definite covariance matrices, respectively:  $Q_\eta$ ,  $Q_x$ , and  $R$ . The matrices  $A$  to  $M$  are calculated by numeric linearization, using the SOAPP for a set of 49 base points covering the power-setting range and indexed with  $PT4$  values ranging from 23 to 260 lb/in.<sup>2</sup> The matrices are updated in flight, based on the  $PT4$  index nearest to the measured value of  $PT4$  with some hysteresis to avoid undesired switching.

With model (6),  $\eta$  and  $x$  are estimated simultaneously using the asymptotic KF (see, for instance, Refs. 7 or 8)

$$\begin{bmatrix} \dot{\hat{x}} \\ \dot{\hat{\eta}} \end{bmatrix} = F \begin{bmatrix} \hat{x} \\ \hat{\eta} \end{bmatrix} + Gu + K \left( y - H \begin{bmatrix} \hat{x} \\ \hat{\eta} \end{bmatrix} \right) \quad (7)$$

$$F := \begin{bmatrix} A & L \\ 0 & 0 \end{bmatrix}, \quad G := \begin{bmatrix} B \\ 0 \end{bmatrix}, \quad H := [C:M] \quad (8)$$

$$K := \begin{bmatrix} K_x \\ K_\eta \end{bmatrix} = PH^T R^{-1}, \quad Q := \begin{bmatrix} Q_x & 0 \\ 0 & Q_\eta \end{bmatrix}$$

where  $P$  is the steady-state solution of the Riccati<sup>8</sup> differential equation associated with the covariance matrix of the estimation error calculated from

$$FP + PF^T + Q - PH^T R^{-1} HP = 0 \quad (9)$$

$R$  is estimated from the sample statistics of the output measurements. The submatrix  $Q_x$  can be associated with the input noise. The entries of the submatrix  $Q_\eta$ , which has no physical meaning in this context, are used as "tuning parameters" empirically adjusted to give a good compromise between time response and noise rejection. The design gives as a result 49 matrices  $K \in \mathbb{R}^{8 \times 5}$  (one for each point indexed by  $PT4$ ) that are stored together with the matrices  $A$  to  $M$ .

#### Optimization Model of the PSC Algorithm

The optimization model of the PSC algorithm (see Fig. 2) is a simplified steady-state model of the propulsion system called the compact propulsion system model (CPSM). It combines two submodels: the compact inlet model (CIM) and the compact engine model (CEM). The subsonic CIM calculates the  $DINL$  and  $PT2$  as functions of the Mach number, corrected fan airflow ( $WCFAN$ ), and  $P_{amb}$ . At subsonic flight conditions, the inlet geometry is scheduled and is not modified by the PSC algorithm. The CEM comprises the engine and the nozzle. Part of the CEM is the steady-state variable model (SSVM), which consists of a piecewise linearization of the steady-state formulation of the aerothermodynamic equa-

tions. Each of the SSVMs local models relates the vector  $\eta$  [defined in Eq. (2)] with small increments in  $Z$ ,  $Y$ , and  $U$  [see definitions in Eq. (3)] around a base point in the following way:

$$z = \begin{bmatrix} y \\ y_{aux} \end{bmatrix} = \begin{bmatrix} G_y \\ G_{aux} \end{bmatrix} u + \begin{bmatrix} H_y \\ H_{aux} \end{bmatrix} \eta \quad (10)$$

where:  $G_y \in \mathbb{R}^{5 \times 6}$ ;  $G_{aux} \in \mathbb{R}^{7 \times 6}$ ;  $H_y \in \mathbb{R}^{5 \times 5}$ ;  $H_{aux} \in \mathbb{R}^{7 \times 5}$ . The relationship between the incremental input vector  $u$  and the incremental measurable vector  $y$  can thus be written as

$$y = G_y u + H_y \eta \quad (11)$$

Equation (11) is the steady-state version of the SVM [Eq. (4)] and can be determined from the latter by equating the time derivatives to 0. Matrices  $G_y$ ,  $G_{aux}$ ,  $H_y$ , and  $H_{aux}$  are calculated off-line based on the SOAPP for each of the discrete tabulated base points. Their values are also tabulated and are used to determine, by interpolation, the current matrices of model (10) each time the base point is updated. The interpolation is performed using as indices the variables  $PT4$  and  $PT6$ . The last estimation of  $\eta$  is introduced into the model (10), which is used by the optimization process to determine the new trims to be sent to the actuators (see Fig. 2). Notice that  $\eta$  is an intermediate entity used only to predict  $z$  for a given  $u$  inside the optimization process.

### Observability Conditions and Equivalence Between Biases and EDPs

#### Observability of the EDPs

A necessary condition (see, for instance, Ref. 8) for the existence of the asymptotic KF [Eqs. (7–9)] is the observability of model (6) (consult Ref. 9 for a definition of the notion of observability). Since the observability of model (6) can be tested directly from its matrices, the following question may be addressed: which is the largest dimension of  $\eta$  compatible with its identifiability with the steady-state Kalman filter (7)? We prove that the dimension of  $\eta$  must be less than or equal to the number of available output measurements. For this, we use the following result proven in Appendix A.

*Proposition 1.* If, given the model (6) with  $n$  the dimension of  $x$ ,  $p$  the dimension of  $\eta$ , and  $m$  the dimension of  $y$ , the matrix

$$S = \begin{bmatrix} A & L \\ C & M \end{bmatrix} \quad (12)$$

is such that  $\text{rank}^*(S) < n + p$ , then, model (6) is not observable.

Now, since  $S$  has at most  $\text{rank } n + m$ , a necessary condition for model (6) to be observable is that, according to Proposition 1,  $n + m \geq n + p$  or, equivalently,  $m \geq p$ , which implies that one needs at least as many measured outputs as the dimension of the vector  $\eta$ . The latter condition is satisfied by the engine's model (6) [or (4)] with  $p = m = 5$ , implying that no extra estimable components can be added to the vector  $\eta$  to quantify an off-nominal engine condition, unless more measurements are made available.

#### Equivalence Between Biases and EDPs

Biases may be present either in the input or the output measured variables. With the present measurement system, the biases' effects cannot be distinguished from those produced by "equivalent" EDPs. We show this for the steady-state model (10). The proof for the actual dynamic model (4) follows similar lines and may be consulted in Ref. 10.

Consider an input bias vector  $v$  and an output bias vector  $\gamma$ . The input-output relationship [Eq. (11)] is thus written as

$$y = H_y \eta + G_y u + G_y v + \gamma \quad (13)$$

From Eq. (13) one sees that, at least in steady state, biases  $\nu$  and  $\gamma$  cannot be distinguished from an (apparent) equivalent increment in  $\eta$  given by

$$\eta_{eq} = H_y^{-1}(G_y \nu + \gamma) \quad (14)$$

The invertibility of the matrix  $H_y$  is clearly satisfied in practice; otherwise, it can be seen from Eq. (13) that the chosen EDPs will not have independent effects on the measured outputs. Equation (14) explains how biases in measurements alter the estimated EDPs. Moreover, it warns us that any "estimated" off-nominal condition may only be the effect of a particular set of biases.

Given the equivalence between biases and EDPs, with Proposition 1 and subsequent discussion, one concludes that the biases cannot be estimated unless more unbiased measures are made available.

#### Estimation Errors Induced by the Biases

As shown previously, the effects of biases in the measurements cannot be distinguished from increments on the EDPs. Any estimation algorithm will then be unable to discern whether the apparent EDPs are the consequence of a real departure of the engine from its nominal behavior or whether they are simply caused by biases in the measurements. Since biases cannot be estimated with the present measurement system, the estimates are affected by an error that is impossible to determine (or estimate) unless the biases are known a priori. We now proceed to calculate the errors induced by the measurement biases.

We call  $\eta_{eq}(\nu)$  and  $\eta_{eq}(\gamma)$  the apparent increments of  $\eta$  (giving rise to corresponding EDP estimation errors) induced, respectively, by biases in the inputs and biases in the measured outputs. Based on Eq. (14), they are defined as

$$H_y \eta_{eq}(\nu) = G_y \nu \Rightarrow \eta_{eq}(\nu) := H_y^{-1} G_y \nu \quad (15)$$

$$H_y \eta_{eq}(\gamma) = \gamma \Rightarrow \eta_{eq}(\gamma) := H_y^{-1} \gamma \quad (16)$$

They clearly satisfy:  $\eta_{eq}(\nu) + \eta_{eq}(\gamma) = \eta_{eq}$ . The estimate,  $\hat{y}_{aux}$ , calculated using the optimization model (10), is

$$\hat{y}_{aux} = G_{aux} u + H_{aux} \hat{\eta} \quad (17a)$$

$$\hat{\eta} := \eta_{ap} + \tilde{\eta} \quad (17b)$$

$$\eta_{ap} := \eta + \eta_{eq} \quad (17c)$$

where  $\hat{\eta}$  is the estimation provided by the KF. Notice that when  $\eta_{eq} = 0$ , the "apparent" value of  $\eta$  is  $\eta$  itself, i.e.,  $\eta_{ap} = \eta$ . Only in this case the estimation error is  $\tilde{\eta} := \hat{\eta} - \eta$ .

On the other hand, the actual (but unknown) value of  $y_{aux}$  as a function of the unknown bias  $\nu$  is given by

$$y_{aux} = G_{aux}(u + \nu) + H_{aux} \eta \quad (18)$$

The estimation error  $\bar{y}_{aux} := \hat{y}_{aux} - y_{aux}$  can be obtained subtracting (18) from (17a). Its component due to the input measurement biases and that due to the output measurement biases are, respectively

$$\bar{y}_{aux}(\nu) = [H_{aux} H_y^{-1} G_y - G_{aux}] \nu \quad (19)$$

$$\bar{y}_{aux}(\gamma) = H_{aux} H_y^{-1} \gamma \quad (20)$$

Equations (19) and (20) are used in the next section to evaluate the biases' effects for a particular engine.

#### Quantitative Study of the Biases' Effects

The results of the previous section are used to measure the influence of the biases on the estimation errors of the auxiliary

variables for the F100 engine of the F15 PSC-test bed aircraft at NASA Dryden. We investigate 1) which biases are most influential and, thus, where to concentrate efforts to improve the instrumentation; and conversely, 2) which of the estimated propulsion variables are affected the most by the biases.

The errors induced by the biases on the calculated auxiliary variables are used as a measure of the effectiveness of the estimation process and the measurement system. Those variables were chosen since they are the ultimate estimate variable transmitted to the optimization process. The auxiliary variables are normalized to allow the comparison of magnitudes of different physical natures under a single scale. The normalizing factors were selected equal to what experience shows to be a typical excursion of the value of each parameter during PSC flight testing. Those magnitudes are stated in Appendix B. By plotting normalized auxiliary variables, it is possible to discern between "big" and "small" effects of the biases. For instance, a big (small) bias effect is one that produces a deviation in the corresponding auxiliary variable which is, "somewhat," comparable to (small with respect to) a typical excursion—the normalizing factor—in that variable. The same notions of big or small can similarly be applied to the biases themselves. In what follows, the ratio between the normalized deviation of an auxiliary variable, and the normalized bias that produces the deviation will be called amplifying factor of the bias with respect to the specific auxiliary variable.

The study is carried out over the whole range of  $PT4$  of the reference flight conditions without afterburner. Given the close relationship between  $PT4$  and the engine's power, the results illustrate the influence of the power setting on the accuracy of the estimation. All the magnitudes are expressed in percentages of the normalizing factors.

#### Effects of the Input Biases

Relationship (19) is used for each local model, indexed by  $PT4$ , to study the effects of the input biases over the estimation errors of the auxiliary variables. Biases of 1% (with respect to the corresponding normalizing factor) were considered for each input, and their effects on  $y_{aux}$  plotted as a function of  $PT4$ .

The results show a very important influence of a bias on  $WF$  (see Fig. 3a). Its effect may be orders of magnitude bigger

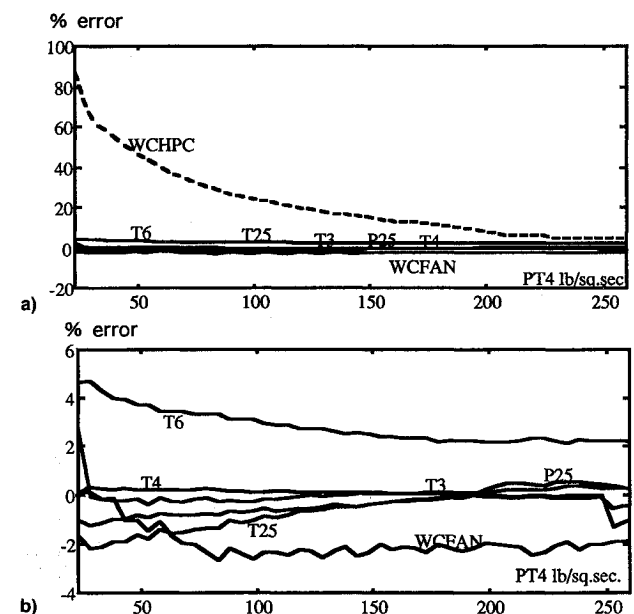


Fig. 3 Normalized auxiliary variable estimation errors resulting from a 1% bias in  $WF$  as a function of  $PT4$ : a) involving  $WCHPC$  and b) enlarged scale not involving  $WCHPC$ .

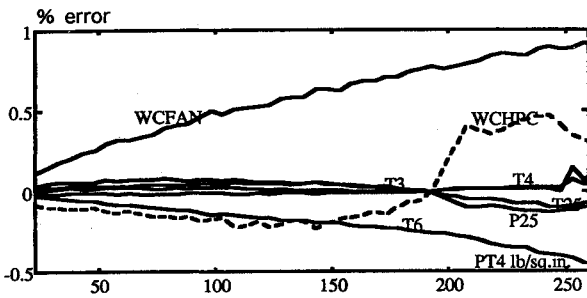


Fig. 4 Normalized auxiliary variable estimation errors resulting from a 1% bias in *AJ* as a function of *PT4*.

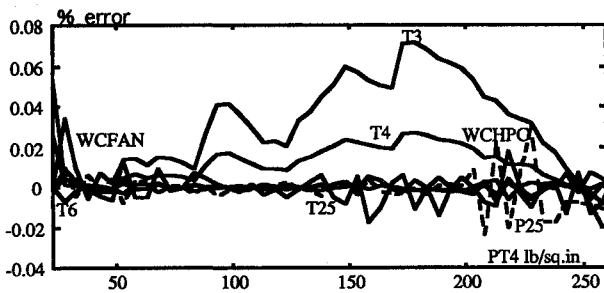


Fig. 5 Normalized auxiliary variable estimation errors resulting from a 1% bias in *RCVV* as a function of *PT4*.

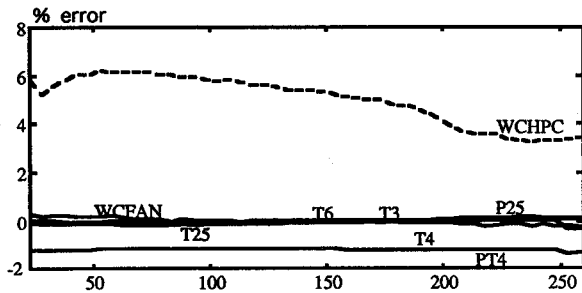


Fig. 6 Normalized auxiliary variable estimation errors resulting from a 1% bias in *FTIT* as a function of *PT4*.

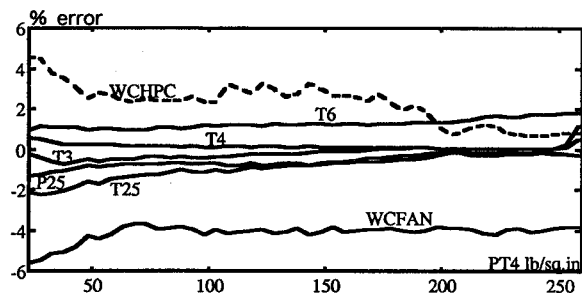


Fig. 7 Normalized auxiliary variable estimation errors resulting from a 1% bias in *PT6* as a function of *PT4*.

than those induced by the rest of the inputs. Notice, in particular, the important effects on corrected high-pressure compressor airflow (*WCHPC*) which attains amplifying factors as big as 20 at middle powers. From the enlargement of Fig. 3a given in Fig. 3b, one sees that *TT6* and *WCFAN*, with amplifying factors bigger than 2, are also considerably affected. Biases in *AJ* are mainly perceived on the estimation of *WCFAN* (see Fig. 4). Unlike the effects of the bias in *WF*, the influence of a bias in *AJ* increases with the power level. The other input biases have no significant incidence on the estimates. Figure

5 illustrates, for instance, the effects of a bias on *RCVV* which attains amplification factors much smaller than unity.

In terms of the possible biases affecting the inputs, we thus conclude that 1) gas generator gas flow *WF* is largely the most critical input variable and its effects are particularly strong for low and medium power settings; 2) the biases in *CIVV* and *RCVV* do not have any significant influence on the estimated variables; 3) biases in *AJ* have a significant influence on the estimation of *WCFAN*; and 4) only the estimates of *WCHPC*, *WCFAN*, and *TT6* can be considered to be affected by the input biases.

**Effects of the Output Biases**

An analog study for the output variables, conducted by using Eq. (20), shows amplifying factors greater than 4 for *FTIT* and afterburner inlet total pressure (*PT6*) at middle- and high-power settings (see Figs. 6 and 7). The biggest effects are those produced on *WCHPC* by a bias in *FTIT* (amplifying factor of 4 to 6). Similar plots for the rest of the input variables can be found in Ref. 10, where it is also shown that *PT4* has, in the worst case (with respect to *TT3*), an amplification factor smaller than 1. Given the generally good quality of the measurements of *N1* and *N2*, we are not concerned by the effects of their biases.

In terms of possible biases affecting the output, we conclude that: 1) biases in *FTIT* and *PT6* have a noticeable effect on the estimations; and 2) as with the input biases, the estimations most affected are *WCHPC* and *WCFAN* (see Figs. 6 and 7). To a lesser extent, *TT6*, *TT4*, and *TT3* are also affected.

**Concluding Remarks**

The EDP estimates do not necessarily quantify the engine's off-nominal behavior. For instance, it is impossible to distinguish the effects produced on those estimates by an off-nominal engine condition from those caused by measurement biases. For PSC application, a given engine off-nominal characterization needs to be evaluated through the effects that biases may have on the predictions provided by the optimization model. The accuracy with which the latter predicts the output variables is the ultimate measure of the effectiveness of the estimation process. Here, the errors induced by the biases on the calculated auxiliary variables are used as a measure of the effectiveness of the estimation process and the measurement system. It is thus determined that the most critical measurements are *WF*, *AJ*, *FTIT*, and *PT6*. Unknown biases on those measurements may have a strong effect on the optimization through a wrong estimation of the engine's variables. Among these variables, the most affected are the *WCHPC*, the *WCFAN*, and the afterburner inlet total temperature (*TT6*). The strong influence of the biases on the airflow estimates is of special importance, inasmuch as those estimates are key for the thrust calculation and, consequently, can sensibly affect the subsequent performance optimization.

The open-loop nature of PSC makes it very sensitive to model-engine mismatches and, in particular, to unknown input or measurement biases. An apparent estimated engine deviation may only be the effect of unknown biases. Under these conditions, trying to improve the performance of an engine in apparently "good shape" (which in fact is not) could lead to inadvertent violations of the optimization constraints and eventually to the activation of the engine's safety guard devices. Conversely, if the engine is better than it seems through the estimation process, a too conservative control will not take advantage of the engine's actual capabilities. Consequently, it is conceivable in this case that the PSC system will issue commands leading to a worse performance than the one obtained with the nominal model in the nonadaptive case. This conclusion strongly demonstrates the need to develop new adaptive performance optimization techniques less sensitive to an a priori engine model on which are based on the feedback of an actual performance measure.

### Appendix A: Proof of Proposition 1

Using standard results of the observability theory of linear systems,<sup>9</sup> it can be readily shown that model (6) is completely observable, if and only if the matrix

$$O := \begin{bmatrix} C & M \\ CA & CL \\ CA^2 & CAL \\ \vdots & \vdots \\ CA^{n+p-1} & CA^{n+p-2}L \end{bmatrix}$$

has rank  $n + p$ . But, since as it can be easily shown

$$O = \begin{bmatrix} I_m & 0 \\ 0 & C \\ 0 & CA \\ \vdots & \vdots \end{bmatrix} \begin{bmatrix} C & M \\ A & L \end{bmatrix}$$

for  $\text{rank}(O) = n + p$  it is necessary that  $S$  in Eq. (12) be such that:  $\text{rank}(S) \geq n + p$ .

### Appendix B: Normalizing Factors

Input variables

WF: 2000.0 lb/h,  $A_j$ : 20 in.<sup>2</sup>, CIVV: 5 deg, RCVV: 5 deg

Output variables

N1: 1000 rpm, N2: 1000 rpm, PT4: 50 lb/in.<sup>2</sup>

FTIT: 200°F, PT6: 5 lb/in.<sup>2</sup>

Auxiliary variables

TT6: 200°F, WCFAN 20 lb/s, PT2.5: 5 lb/in.<sup>2</sup>

TT2.5: 50.0°F, TT3: 100.0°F, TT4: 200.0°F

WCHPC: 2.0 lb/s

### Acknowledgments

This work was done while the author was a Senior Research Associate of the National Research Council at NASA Dryden Flight Research Facility. The author is indebted to Glenn Gilyard for insightful discussions and invaluable technical advice. Special thanks are in order to John Orme for his assistance in obtaining the data and with the different computational problems.

### References

<sup>1</sup>Luppold, R. H., Gallops, G. L. K., and Roman, J. R., "Estimating In-Flight Engine Performance Variations Using Kalman Filter Concepts," AIAA Paper 89-2584, July 1989.

<sup>2</sup>Gilyard, G. B., and Orme, J. S., "Subsonic Flight Test Evaluation of a Performance Seeking Control Algorithm on an F-15 Airplane," AIAA Paper 92-3743, July 1992; also NASA TM-4400, Aug. 1992.

<sup>3</sup>Nobbs, S. G., Jacobs, S. W., and Donahue, D. J., "Development of the Full-Envelope Performance Seeking Control Algorithm," AIAA Paper 92-3748, July 1992.

<sup>4</sup>Orme, J. S., and Gilyard, G. B., "Subsonic Flight Test Evaluation of a Propulsion System Parameter Estimation Process for the F100 Engine," AIAA Paper 92-3745, July 1992; also NASA TM-4426, Nov. 1992.

<sup>5</sup>Orme, J. S., and Gilyard, G. B., "Preliminary Supersonic Flight Test Evaluation of Performance Seeking Control," AIAA Paper 93-1821, June 1993.

<sup>6</sup>Alag, G. S., and Gilyard, G. B., "A Proposed Kalman Filter Algorithm for Estimation of Unmeasured Output Variables for an F100 Turbofan Engine," AIAA Paper 90-1920, July 1990; also NASA TM-4234, Oct. 1990.

<sup>7</sup>Kalman, R. E., and Bucy, R. S., "New Results in Linear Filtering and Prediction Theory," *Journal of Basic Engineering Transactions of the ASME*, Series D, No. 3, 1961, pp. 95-108.

<sup>8</sup>Kailath, T., *Lectures on Wiener and Kalman Filtering*, CISM Courses and Lectures No. 140, International Centre for Mechanical Sciences, Springer-Verlag Wien, New York, 1981.

<sup>9</sup>Wolovich, W. A., *Linear Multivariable Systems*, Applied Mathematical Sciences No. 11, Springer-Verlag, New York, 1974.

<sup>10</sup>España, M. D., and Glenn, G. B., "On the Estimation Algorithm of the Performance Seeking Controller for Turbofan Engines," NASA TM-4551, Nov. 1993.